

Efficient methods for computing integrals in electronic structure calculations

Hisashi Kohashi¹, Kosuke Sugita¹, Masaaki Sugihara¹ and Takeo Hoshi²

¹ Aoyama Gakuin University, 5-10-1 Fuchinobe, Chuo-ku, Sagami-hara-shi, Kanagawa 252-5258, Japan

² Tottori University, 4-101 4-101 Koyama-cho Minami, Tottori, 680-8552, Japan

E-mail ksk.sgt@gmail.com

Received

Abstract

Efficient methods are proposed, for computing integrals appearing in electronic structure calculations. The methods consist of two parts: the first part is to represent the integrals as contour integrals and the second one is to evaluate the contour integrals by the Clenshaw-Curtis quadrature. The efficiency of the proposed methods is demonstrated through numerical experiments.

Keywords electronic structure calculation, contour integral, Clenshaw-Curtis quadrature

Research Activity Group Scientific Computation and Numerical Analysis

1. Introduction

In this paper, we propose efficient methods for computing the following integrals appearing in electronic structure calculations [1, 2]:

$$I(\mu, \tau) \equiv -\frac{1}{\pi} \lim_{\eta \downarrow +0} \text{Im} \int_{-\infty}^{\infty} W(x; \mu, \tau) G(x + i\eta) dx, \quad (1)$$

where $G(z)$ is the Green's function which is defined as

$$G(z) = \mathbf{b}^* (zI - H)^{-1} \mathbf{b}, \quad (2)$$

where \mathbf{b} is a vector and H is the so-called Hamiltonian matrix (a Hermitian matrix), and $W(x; \mu, \tau)$ is the Fermi-Dirac function:

$$W(x; \mu, \tau) = \frac{1}{1 + \exp\left(\frac{x - \mu}{\tau}\right)},$$

where μ is a real number, and τ is a small positive number. The Green's function $G(z)$ is expanded as follows:

$$G(z) = \sum_{j=1}^N \frac{c_j}{z - \lambda_j}, \quad (3)$$

where N is the order of H , c_j ($j = 1, 2, \dots, N$) are non-negative real numbers, and λ_j ($j = 1, 2, \dots, N$) are the eigenvalues (real numbers) of H , which correspond to the energy levels in the material. We assume that λ_j 's are labeled in increasing order: $\lambda_1 < \lambda_2 < \dots < \lambda_N$. We also assume that a lower estimate for the smallest eigenvalue, λ_1 , is known, although λ_j ($j = 1, 2, \dots, N$) are unknown.

In [2], the trapezoidal rule is applied to evaluate the integral in $I(\mu, \tau)$, by taking η as a very small number, and by setting the interval of integration adequately wide. It is evident that many sampling points are necessary, since $G(z)$ has many poles on the real axis. However, due to a limited time of computation, the number of the sampling points is not as many as supposed to be. Therefore, the

accuracy of the computed results is not enough.

In this paper, we propose two methods for computing $I(\mu, \tau)$ efficiently, both of which consist of two parts: the first part is to represent the integrals as contour integrals and the second one is to evaluate the contour integrals by the Clenshaw-Curtis quadrature.

The paper is organized as follows. In Sec. 2, we introduce one of the proposed methods, which we call Method 1, and give a numerical example. Subsequently, in Sec. 3, we present another method, which we call Method 2, together with a numerical example. In Sec. 4, we develop a method for computing $I(\mu, \tau)$ for many distinct values of μ , which situation sometimes arises. Finally, in Sec. 5, we make concluding remarks.

2. Method 1

It is easily verified that $I(\mu, \tau)$ is equal to $\sum_j c_j W(\lambda_j; \mu, \tau)$. Thus, by setting the contour C as a simply closed curve which encloses all the poles of $G(z)$ but does not of $W(z)$ (Fig. 1), the contour integral representation of I is obtained as follows:

$$I(\mu, \tau) = \frac{1}{2\pi i} \int_C W(z; \mu, \tau) G(z) dz. \quad (4)$$

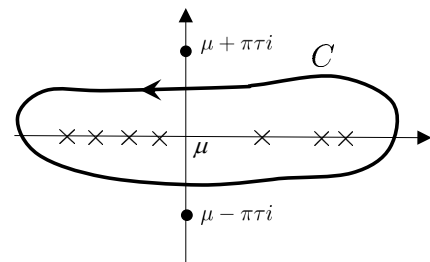


Fig. 1. The contour C (×: the poles of $G(z)$) (•: the poles of $W(z; \mu, \tau)$)

It is expected that we will perform the numerical integration efficiently with this contour integral, because we can set the contour far from the poles of $G(z)$ on the real axis.

Taking account of easiness of numerical integration, we now set the contour of the integral as $L_1 + L_2 + L_3 + C_4$ illustrated in Fig. 2, where

- (a) ℓ is a real number that is smaller than the smallest pole of $G(z)$, i.e., λ_1 (note that the possibility of setting up this number is guaranteed by the assumption that a lower estimate for λ_1 is known), and also such that $W(\ell; \mu, \tau) \approx 1$, i.e., $|W(\ell; \mu, \tau) - 1|$ is small enough (in the numerical examples below, we set $|W(\ell; \mu, \tau) - 1| \leq 10^{-40}$);
- (b) u is a real number such that $W(u; \mu, \tau) \approx 0$ (in the numerical examples below, we set $|W(u; \mu, \tau)| \leq 10^{-40}$);
- (c) $L_1 = [u + (\pi\tau/2)i, \ell + (\pi\tau/2)i]$;
- (d) $L_2 = [\ell + (\pi\tau/2)i, \ell - (\pi\tau/2)i]$;
- (e) $L_3 = [\ell - (\pi\tau/2)i, u - (\pi\tau/2)i]$;
- (f) C_4 is a curve connecting the points $u - (\pi\tau/2)i$ and $u + (\pi\tau/2)i$ and such that $L_1 + L_2 + L_3 + C_4$ encloses all the poles of $G(z)$.

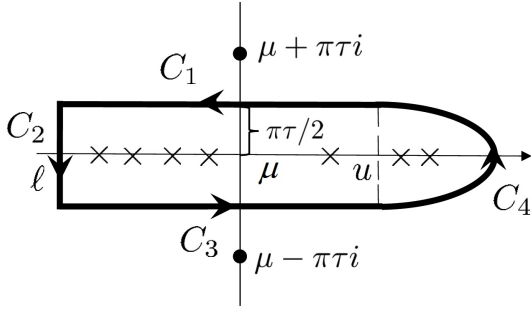


Fig. 2. The contour $L_1 + L_2 + L_3 + C_4$ (\times : the poles of $G(z)$, \bullet : the poles of $W(z)$)

Then, denoting $W(z; \mu, \tau)G(z)$ by $F(z; \mu, \tau)$, we have

$$\begin{aligned} \frac{1}{2\pi i} \int_{L_1} F(z; \mu, \tau) dz + \frac{1}{2\pi i} \int_{L_3} F(z; \mu, \tau) dz \\ = -\frac{1}{\pi} \int_{\ell}^u \operatorname{Im} F(x + \frac{\pi\tau}{2}i; \mu, \tau) dx, \end{aligned}$$

$$\frac{1}{2\pi i} \int_{L_2} F(z; \mu, \tau) dz \approx -\frac{1}{\pi} \int_0^{\frac{\pi\tau}{2}} \operatorname{Re} G(\ell + yi) dy,$$

$$\frac{1}{2\pi i} \int_{C_4} F(z; \mu, \tau) dz \approx 0.$$

Thus, we obtain

$$I(\mu, \tau) \approx I_h + I_v$$

where

$$I_h = -\frac{1}{\pi} \int_{\ell}^u \operatorname{Im} F(x + \frac{\pi\tau}{2}i; \mu, \tau) dx, \quad (5)$$

$$I_v = -\frac{1}{\pi} \int_0^{\frac{\pi\tau}{2}} \operatorname{Re} G(\ell + yi) dy. \quad (6)$$

For calculation of I_h and I_v we adopt the Clenshaw-Curtis quadrature [3], because the integrands are analytic over the intervals of integration.

Numerical example 1 We consider the case where the Green's function is given by

$$G(z) = \sum_{j=1}^{4686} \frac{1}{z - \lambda_j},$$

which appears in an electronic structure calculation of a nanoscale amorphous-like conjugated polymer [4]. The values of $\lambda_1, \lambda_2, \dots, \lambda_{4686}$ ($\lambda_1 \simeq -1.16, \lambda_{4686} \simeq 5.58$) are given on the website [5] as the data set ‘‘APF4686’’. (The actual computation of $G(z)$ is done by using the expression (2), that is, by solving the large system of linear equations $(zI - H)\mathbf{x} = \mathbf{b}$, which leads to relatively large numerical errors. Since we here concentrate on examining numerical errors caused by the numerical integration, we give $G(z)$ as the rational expression as above, the computation of which produces small numerical errors.)

We first set μ as

$$\mu = (\lambda_{2343} + \lambda_{2344})/2 = -0.3917431575916144, \quad (7)$$

where

$$\lambda_{2343} = -0.4258775547956950,$$

$$\lambda_{2344} = -0.3576087603875338,$$

and $\tau = 0.01$. In this case, the exact value of $I(\mu, \tau)$ is $2342.992785654893 \dots$. We evaluate the integrals I_h and I_v with the Clenshaw-Curtis quadrature, setting $\ell = -1.5, u = 0.6$. For I_v , whose integrand has no poles near the interval of integration, a very rapid convergence of the Clenshaw-Curtis quadrature is observed: the relative error 10^{-15} is attained with 7 sampling points. For I_h , whose integrand has many poles near the interval of integration, the convergence behavior is shown in Fig. 3. Exponential convergence is observed, as expected from the convergence theory of the Clenshaw-Curtis quadrature.

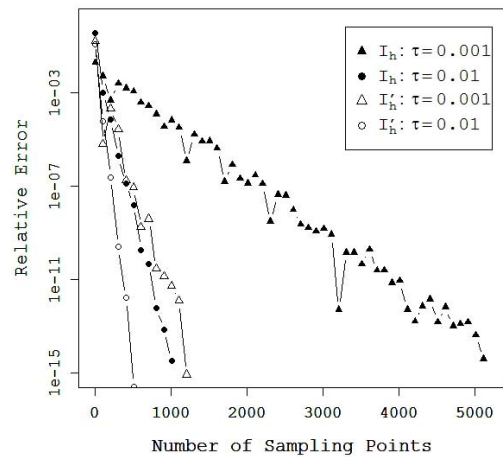


Fig. 3. The convergence behaviors of the Clenshaw-Curtis quadrature for I_h and I'_h

Next, we set μ the same as above and $\tau = 0.001$. The exact value of $I(\mu, \tau)$ is 2343.000000000000... We evaluate I_h and I_v with the Clenshaw-Curtis quadrature, setting $\ell = -1.5, u = -0.3$.

For I_v , the relative error 10^{-15} is achieved with 6 sampling points. For I_h , Fig. 3 shows the convergence behavior. Exponential convergence is observed, which is slower than that of the case of $\tau = 0.01$.

3. Method 2

Fig. 3 shows that Method 1 requires a large number of sampling points, that is, function evaluations for computing the integral I_h , which caused by the proximity of the paths L_1, L_3 to the poles of $W(z)G(z)$. To solve this problem, we take the contour $L'_1 + L'_2 + L'_3 + C'_4$ so that it is far from the poles of $W(z)G(z)$, as shown in Fig.4.

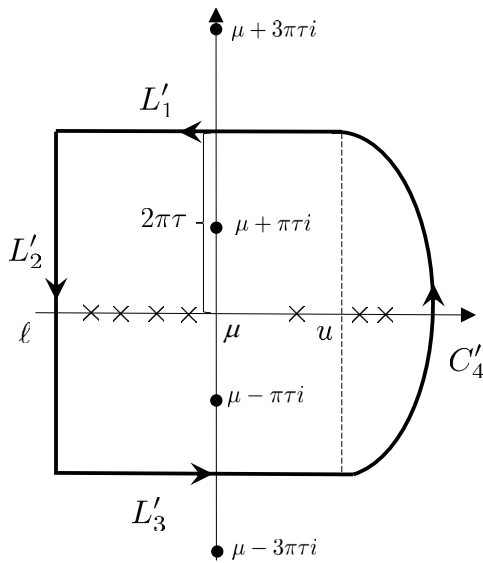


Fig. 4. The contour $L'_1 + L'_2 + L'_3 + C'_4$ (×: the poles of $G(z)$, •: the poles of $W(z)$)

In this setting, we should consider the residues of $W(z; \mu, \tau)$ at $z = \mu \pm \pi\tau i$, thus the contour integral becomes

$$\begin{aligned} & \frac{1}{2\pi i} \int_{L'_1 + L'_2 + L'_3 + C'_4} F(z; \mu, \tau) dz \\ &= I(\mu, \tau) + \text{Res}(F, \mu + \pi\tau i) + \text{Res}(F, \mu - \pi\tau i) \\ &= I(\mu, \tau) - 2\tau \text{Re} G(\mu + \pi\tau i). \end{aligned}$$

Calculating the left-hand side similarly as in Method 1, we obtain

$$I(\mu, \tau) \approx I'_h + I'_v + 2\tau \text{Re} G(\mu + \pi\tau i),$$

where

$$I'_h = -\frac{1}{\pi} \int_{\ell}^u \text{Im} F(x + 2\pi\tau i; \mu, \tau) dx, \quad (8)$$

$$I'_v = -\frac{1}{\pi} \int_0^{2\pi\tau} \text{Re} G(\ell + yi) dy. \quad (9)$$

For evaluation of I'_h and I'_v , we use the Clenshaw-Curtis quadrature.

Numerical example 2 We set $G(z), \mu$, and τ as the same as in Numerical example 1. First, in the case of $\tau = 0.01$, we evaluate the integrals I'_h and I'_v with the Clenshaw-Curtis quadrature, setting $\ell = -1.5, u = 0.6$. For I'_v , the relative error 10^{-15} is attained with 12 sampling points. For I'_h , Fig. 3 shows the convergence behavior of the Clenshaw-Curtis quadrature. Next, in the case of $\tau = 0.001$, we compute the integrals I'_h and I'_v with the Clenshaw-Curtis quadrature, setting $\ell = -1.5, u = -0.3$. For I'_v the relative error 10^{-15} is achieved with 6 sampling points. For I'_h , Fig. 3 shows the convergence behavior of the Clenshaw-Curtis quadrature. We can see that the performance is much improved.

Remark 1 Setting such contour contributes not only to fast computations of integrations, but also to the actual computation of $G(z)$. In fact, the actual computation of $G(z)$ requires to solve the equation $(zI - H)\mathbf{x} = \mathbf{b}$ with Krylov subspace methods such as the COCG method. And it is known that the farther the distances between z and the eigenvalues of H , i.e., λ_j 's, the faster the convergence of Krylov subspace methods in general.

4. Method for computing $I(\mu, \tau)$ with various values of μ

It is often the case that we need to compute $I(\mu, \tau)$ for many distinct values of μ . Computing separately for each value of μ with Method 1 or 2, costs a massive amount of calculation in total. Instead we propose an efficient method based on Method 1. It is supposed here that the range of required μ , say $[\mu_{\min}, \mu_{\max}]$, is known.

In Method 1, it is evident that the computation of $I_h(\mu, \tau)$ for many values of μ causes the massive amount of computation. Hence we reduce the amount of the computation of $I_h(\mu, \tau)$ for many values of μ . The key is to use common ℓ and u (See (5)) in the computation of $I_h(\mu, \tau)$ for many values of μ . In fact, we can use ℓ_{\min} and u_{\max} as the common ℓ and u respectively, where ℓ_{\min} is a real number that is less than or equal to the value of ℓ determined in the case of $\mu = \mu_{\min}$, and u_{\max} is a real number that is greater than or equal to the value of u determined in the case of $\mu = \mu_{\max}$. Then,

$$\begin{aligned} I_h &= -\frac{1}{\pi} \int_{\ell_{\min}}^{u_{\max}} \text{Im} W(x + \frac{\pi\tau}{2}i; \mu, \tau) G(x + \frac{\pi\tau}{2}i) dx. \\ \left(I_v &= -\frac{1}{\pi} \int_0^{\frac{\pi\tau}{2}} \text{Re} G(\ell_{\min} + yi) dy \right) \end{aligned}$$

It follows that the computation of G , which costs a large amount of calculation, is independent of μ . Thus, once we compute I_h for an appropriately large μ and store the computed values of $G(x + (\pi\tau/2)i)$ for reuse, we can immediately obtain the result of I_h for another value of μ , by multiplying the stored values of $G(x + (\pi\tau/2)i)$ by $W(x + (\pi\tau/2)i; \mu, \tau)$, the cost of computation of which is low. This device enables us to compute $I(\mu, \tau)$ for many of distinct μ efficiently.

Numerical example 3 We consider the case where

$G(z)$ is the same as in Numerical example 1 and $\tau = 0.01$. We compute $I(\mu, \tau)$ for

$$\mu = (\lambda_{10} + \lambda_{11})/2 = -1.147817562299727,$$

$$\vdots$$

$$\mu = (\lambda_{4650} + \lambda_{4651})/2 = 3.379941668485607.$$

We apply the Clenshaw-Curtis quadrature to evaluate I_h and I_v with $\ell_{\min} = -1.5, u_{\max} = 6.0$. Note that I_v is the same as in Numerical example 1, for which the Clenshaw-Curtis quadrature attains the relative error 10^{-15} with 6 sampling points. For $\mu = (\lambda_{4650} + \lambda_{4651})/2 = 3.3799\dots$, we compute I_h and store the computed values of $G(z)$. Then we compute I_h for another value of μ , by using the stored value of $G(z)$. Fig. 5 shows the convergence behaviors of the Clenshaw-Curtis quadrature for I_h with $\mu = (\lambda_{10} + \lambda_{11})/2 = -1.1478\dots$, $\mu = (\lambda_{2343} + \lambda_{2344})/2 = -0.39174\dots$ and $\mu = (\lambda_{4650} + \lambda_{4651})/2 = 3.3799\dots$.

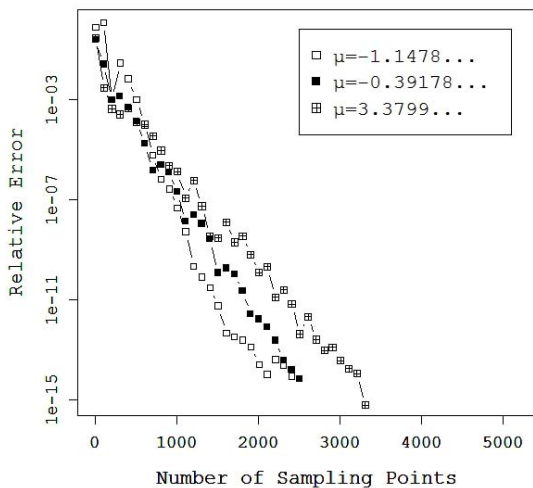


Fig. 5. The convergence behaviors of the Clenshaw-Curtis quadrature for I_h (Note that we compute I_h for $\mu = (\lambda_{10} + \lambda_{11})/2 = -1.1478\dots$, $\mu = (\lambda_{2343} + \lambda_{2344})/2 = -0.39174\dots$, reusing the value of $G(z)$ obtained by the computation in the case of $\mu = (\lambda_{4650} + \lambda_{4651})/2 = 3.3799\dots$)

Remark 2 As for Method 2, we can use a similar device for computing I'_h with various values of μ . In fact, once we compute I'_h for a suitable μ and store the values of $G(x + 2\pi\tau i)$, then we can obtain the results of I'_h for distinct values of μ , by multiplying the stored values of $G(x + 2\pi\tau i)$ by $W(x + 2\pi\tau i; \mu, \tau)$, which does not need much computation.

However, it should be noted that an additional computation of $G(\mu + \pi\tau i)$ is needed for the calculation of I . The fact that Method 2 is faster than Method 1, tells us that Method 2 with this device can be effective when the total cost of computation of $G(\mu + \pi\tau i)$ is not large.

5. Concluding remarks

In this paper, we proposed methods for computing integrals appearing in electronic structure calculations and

showed that the proposed methods are efficient through numerical experiments. We would like to note that the proposed methods are also efficient for the case where the Green's function is given by

$$G(z) = \sum_{j=1}^{4686} \frac{c_j}{z - \lambda_j}$$

where $\{c_j\}$ are uniform random numbers on $[0, 1]$, although the results are not contained here, due to a limited number of pages.

We applied the proposed methods to the Green's function $G(z)$ given as rational expression, but we should treat the Green's function $G(z)$ with (2) using Hamiltonian matrix, which is left for the future work.

References

- [1] R. Takayama, T. Hoshi, T. Sogabe, S.-L. Zhang, and T. Fujiwara, Linear algebraic calculation of the Green's function for large-scale electronic structure theory, *Phys. Rev. B*, **73** (2006), 165108, 1-9.
- [2] H. Teng, T. Fujiwara, T. Hoshi, T. Sogabe, S.-L. Zhang, S. Yamamoto, Efficient and accurate linear algebraic methods for large-scale electronic structure calculations with nonorthogonal atomic orbitals, *Physical Review B*, **83** (2011), 165103, 1-12.
- [3] Lloyd N. Trefethen, *Approximation Theory and Approximation Practice*, SIAM, Oxford, 2013.
- [4] T. Hoshi, S. Yamamoto, T. Fujiwara, T. Sogabe, S.-L. Zhang, An order- N electronic structure theory with generalized eigenvalue equations and its application to a ten-million-atom system, *J. Phys.: Condens. Matter* **24** (2012), 165502, 1-5.
- [5] <http://www.elses.jp/matrix/>